Molecules and Cells

Phosphoserine Phosphatase Promotes Lung Cancer Progression through the Dephosphorylation of IRS-1 and a Noncanonical L-Serine-Independent Pathway

Seong-Min Park[1,6,7], Eun-Hye Seo[3,4,7], Dong-Hyuck Bae[3,4,7], Sung Soo Kim[5,6,7], Jina Kim[1,3], Weiwei Lin[5,6], Kyung-Hee Kim[5,6], Jong Bae Park[5,6], Yong Sung Kim[3,4], Jinlong Yin[2,5,6,*], and Seon-Young Kim[1,4,*]

[1]Personalized Genomic Medicine Research Center, Korea Research Institute of Bioscience & Biotechnology (KRIBB), Daejeon 34141, Korea, [2]Henan and Macquarie University Joint Centre for Biomedical Innovation, School of Life Sciences, Henan University, Kaifeng 475004, China, [3]Genome Editing Research Center, KRIBB, Daejeon 34141, Korea, [4]Department of Bioscience, University of Science and Technology, Daejeon 34113, Korea, [5]Department of Cancer Biomedical Science, Graduate School of Cancer Science and Policy, National Cancer Center, Goyang 10408, Korea, [6]Research Institute, National Cancer Center, Goyang 10408, Korea, [7]These authors contributed equally to this work.
*Correspondence: kimsy@kribb.re.kr (SYK); jly24063@ncc.re.kr (JY)
https://doi.org/10.14348/molcells.2019.0160
www.molcells.org

Phosphoserine phosphatase (PSPH) is one of the key enzymes of the L-serine synthesis pathway. PSPH is reported to affect the progression and survival of several cancers in an L-serine synthesis-independent manner, but the mechanism remains elusive. We demonstrate that PSPH promotes lung cancer progression through a noncanonical L-serine-independent pathway. PSPH was significantly associated with the prognosis of lung cancer patients and regulated the invasion and colony formation of lung cancer cells. Interestingly, L-serine had no effect on the altered invasion and colony formation by PSPH. Upon measuring the phosphatase activity of PSPH on a serine-phosphorylated peptide, we found that PSPH dephosphorylated phospho-serine in peptide sequences. To identify the target proteins of PSPH, we analyzed the protein phosphorylation profile and the PSPH-interacting protein profile using proteomic analyses and found one putative target protein, IRS-1. Immunoprecipitation and immunoblot assays validated a specific interaction between PSPH and IRS-1 and the dephosphorylation of phospho-IRS-1 by PSPH in lung cancer cells. We suggest that the specific interaction and dephosphorylation activity of PSPH have novel therapeutic potential for lung cancer treatment, while the metabolic activity of PSPH, as a therapeutic target, is controversial.

Keywords: IRS-1, L-serine independent pathway, lung cancer, phosphoserine phosphatase

INTRODUCTION

Phosphoserine phosphatase (PSPH), a haloacid dehalogenase containing a conserved N-terminal DXDXT motif, is known to catalyze the reaction from phospho-L-serine to L-serine (Borkenhagen and Kennedy, 1958; Collet et al., 1997; 1998; 1999; Neuhaus and Byrne, 1958; Strunck et al., 2001; Wood et al., 1996). PSPH is a key metabolic enzyme of the L-serine synthesis pathway that converts 3-phosphoglycerate (3-PG) into L-serine using three enzymes, 3-phosphoglycerate

Received 17 July, 2019; accepted 29 July, 2019; published online 19 August, 2019

eISSN: 0219-1032

dehydrogenase (PHGDH), phosphoserine aminotransferase (PSAT1), and PSPH (Lund et al., 1985). In humans, L-serine is one of the nonessential amino acids but is needed for cell proliferation; therefore, PSPH is expressed in various tissues and organs, such as lung, brain, heart, kidney and muscle (Bachelor et al., 2011; Kalhan and Hanson, 2012; Strunck et al., 2001). Abnormalities in the PSPH and L-serine synthesis pathways are known to cause various diseases, including neural damage (de Koning et al., 2003; Tabatabaie et al., 2010; van der Linden et al., 2008). L-serine is reported to play roles in cell proliferation and cancer progression (Amelio et al., 2014; Anderson et al., 2012; Locasale, 2013; Tedeschi et al., 2013; Vazquez et al., 2013), and PSPH is also reported to be associated with various cancers, including cutaneous squamous cell carcinoma (SCC), lung, gastric, breast, brain and colon cancers (Bachelor et al., 2011; Hemmati et al., 2003; Herzfeld et al., 1978; Maddocks et al., 2013; Pollari et al., 2011; Shimomura et al., 2004; Tan et al., 2010). Although PSPH is reported to promote tumorigenesis and metastasis through the L-serine synthesis pathway in breast (Pollari et al., 2011) and colon (Herzfeld et al., 1978) cancer, PSPH is also reported to regulate SCC proliferation independent of the L-serine synthesis pathway (Bachelor et al., 2011), but the mechanism remains elusive. Considering that L-serine-dependent PSPH pathway targeted therapy remains ineffective due to alternative resistance mechanisms through the L-serine synthesis pathway (Ross et al., 2017), studying the functional details of the L-serine-independent pathway of PSPH will be useful to understand cancer progression.

Many reports of PSPH dysregulation are associated with non-small-cell lung cancer (NSCLC) (Tan et al., 2010). Lung cancer is known as the leading cause of cancer-related death worldwide, and patients with NSCLC account for ~75% of all lung cancer cases (Siegel et al., 2013). The risk of relapse in NSCLC patients is considerable; for example, 30% to 35% of stage I patients relapse after their initial surgery (Nesbitt et al., 1995; Hoffman et al., 2000). Conventional NSCLC therapy focusing on cancer patient prognosis for therapeutic strategies, such as postoperative adjuvant therapy and conventional histological markers, has been used, but the effectiveness is controversial according to several randomized studies for prognosis determination (Douillard et al., 2006; Pignon et al., 2008; Roselli et al., 2006; Winton et al., 2005). A previous study on the association between PSPH and NSCLC suggested the possibility of PSPH as a biomarker for lung cancer prognosis (Tan et al., 2010). However, the detailed molecular mechanisms of PSPH in lung cancer progression and its therapeutic approaches remain unclear.

In this study, we investigated the association between the PSPH expression level and the prognosis of lung cancer patients. We also examined the lung cancer-related functions of PSPH and especially whether PSPH functions in lung cancer independent of the L-serine synthesis pathway. Then, we tried to identify a novel target of PSPH and uncover its detailed functions for therapeutic approaches. We suggest that PSPH promotes lung cancer progression through noncanonical pathways and that this mechanism can be a novel target for lung cancer treatment.

MATERIALS AND METHODS

Public data analysis

For survival analysis, two public gene expression and clinical information datasets (GSE30219 and GSE37745) were downloaded from the National Center for Biotechnology Information Gene Expression Omnibus (NCBI GEO) database (http://www.ncbi.nlm.nih.gov/geo/). Gene expression data were globally normalized using the Robust Multi-array Average (RMA) method (Fig. 1A). Kaplan-Meier curves shown in Supplementary Figure S1 were obtained by using the SurvExpress program (http://bioinformatica.mty.itesm.mx/SurvExpress). The TCGA data and Oncoprint figures were downloaded from cBioPortal (http://www.cbioportal.org/). All statistical tests were performed using the R programming language (https://www.r-project.org/), and graphs and heatmaps were prepared using Microsoft Excel and R programs.

Cell culture, siRNAs and His-tagged PSPH clone transfection

A549 cells (ATCC) were maintained in complete DMEM medium (Welgene, Korea) at 37°C in a humidified 5% CO_2 incubator. NCI-H1299 cells (Korean Collection for Type Cultures [KCTC], https://kctc.kribb.re.kr/kctc.aspx) were maintained in complete RPMI 1640 medium (Welgene) at 37°C in a humidified 5% CO_2 incubator. Complete media was supplemented with 10% fetal bovine serum (Welgene), 100 U/ml penicillin/streptomycin (Gibco, USA), and 2 mM L-glutamine. To test serine dependency, 0.5 mM serine was added to the growth media.

The siRNA target sequences were designed using the AsiDesigner program and are listed in Supplementary Table S1. For siRNA transfection, 1.5 to 2.0 × 10^5 lung cancer cells were plated into 6-well plates and incubated overnight. The siRNAs or nontargeting controls, at a concentration of 100 nM, were transfected into lung cancer cells using Lipofectamine RNAiMax (Invitrogen, USA) in Opti-MEM media (Gibco). After 24 h of incubation, the media were changed to complete media, and 48 h after transfection, gene knockdown was confirmed by reverse transcription-quantitative polymerase chain reaction (RT-qPCR).

The His-tagged PSPH clone was constructed by PCR and inserted into the pCDH-CMV-MCS-EF1-Puro (System Biosciences, USA) lentiviral vector. An empty vector was used as a control. For viral particle generation, cloned DNAs and MISSION Lentiviral Packaging Mix (Sigma, USA) were transfected into 293T cells using Lipofectamine 2000 (Invitrogen) in Opti-MEM media (Gibco). After 24 h of incubation, the media were changed to complete media. After 24 h and 48 h of incubation, the supernatant containing the virus particles was harvested and concentrated. For viral infection, 1.5 × 10^5 lung cancer cells were added to each well of a 6-well plate and incubated overnight. The concentrated viral supernatant was added to the plated cells, and after overnight incubation, the media were changed to complete media. After 48 h, gene overexpression was confirmed by an immunoblot assay.

RT-qPCR

Total RNA was extracted using the RNeasy Mini Kit (Qiagen, Germany) according to the manufacturer's instructions. Re-

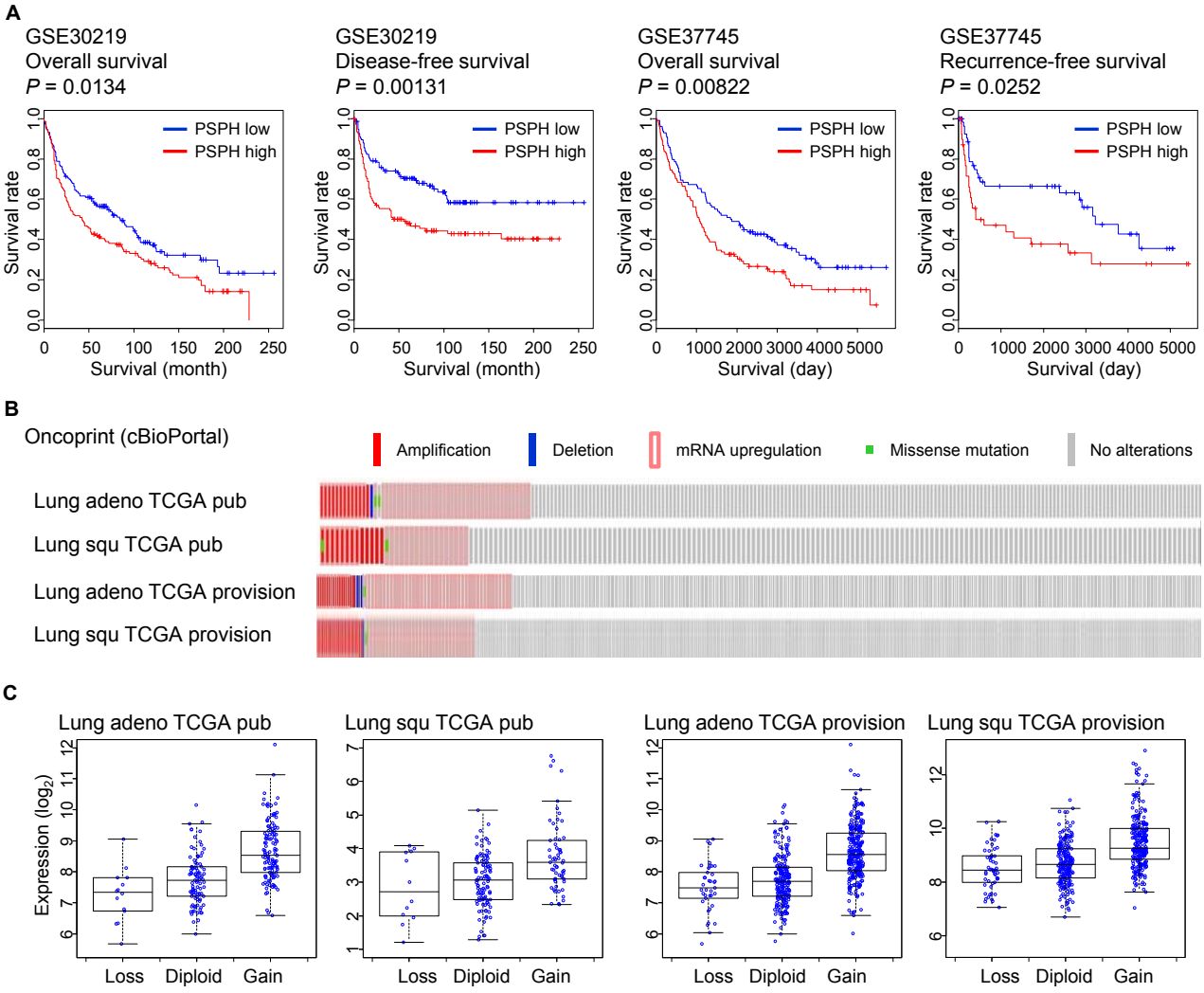

Fig. 1. Promotion of lung cancer progression by PSPH. (A) Prognoses of two groups of lung cancer patients classified by PSPH expression. Red, high expression group; Blue, low expression group. (B) Alteration frequency of PSPH in lung cancer patients (TCGA, cBioPortal, Oncoprint). (C) Correlation between CNA and PSPH expression in lung cancer patients (TCGA).

verse transcription was performed with 1 μg of total RNA as the template and an iScript cDNA Synthesis Kit (Bio-Rad, USA). Quantitative real-time PCRs (qPCRs) were performed in triplicate on a CFX96 Real Time System (Bio-Rad) using iQ SYBR Green Supermix (Bio-Rad). cDNA expression was normalized to that of β-actin, and at least three independent biological replicates were included for each reaction. The primers used for qPCR were designed either manually or with the Primer3 program (http://biotools.umassmed.edu/bioapps/primer3_www.cgi). All primer sequences are listed in Supplementary Table S2.

Immunoblot assay

Total protein samples were prepared in RIPA buffer with protease inhibitor cocktail (Roche, Switzerland) and quantified using Bradford protein assays (Thermo, USA). Equal amounts of the samples were loaded onto an 8% to 12% SDS-PAGE gel, electrophoresed, transferred to an Immobilon-P PVDF membrane (Millipore, USA), and probed with the antibodies listed in Supplementary Table S3. An HRP-conjugated anti-mouse or anti-rabbit IgG antibody (Santa Cruz Biotechnology, USA) was used as the secondary antibody. The bands were detected with SuperSignal West Pico Chemiluminescent Substrate (Thermo).

Histology and IHC staining

For the observation of histologic features, the subcutaneous tissues were removed, fixed with 4% paraformaldehyde for 24 h at 4°C, and stained with hematoxylin (DaKo, USA) and 0.25% eosin (Merck, USA). For the immunohistochemistry (IHC) staining of PSPH and IRS-1, after the antigen retrieval process with citrate buffer (pH 6.0) and endogenous peroxidase blocking with 3% hydrogen peroxide, tissue sections were incubated in the indicated primary antibody overnight at 4°C in a humidified chamber with IHC world antibody diluent buffer. We developed samples using 3,30-diaminobenzi-

dine (DAB; Vector Laboratories, USA) as the chromogen.

For non-small cell lung cancer tissue microarrays (LC121c; US Biomax, USA) staining with PSPH (Sino Biological, China) and pIRS-1 Ser794 (Full Moon BioSystems, USA) antibodies, the antigen retrieval, endogenous peroxidase blocking, primary antibody incubation and DAB development are conducted as same as IHC staining processed.

Invasion assay

Transwell chambers (Corning, USA) were coated with Matrigel Basement Membrane Matrix (BD, USA). Cells were suspended in serum-free media and seeded into the upper chamber at a density of 5.0×10^3 cells per well, and serum-containing media were placed into the lower chamber. After incubation for 4 days, the cells penetrating the pores were stained with crystal violet staining solution (0.5% crystal violet, 3.7% formaldehyde, and 30% ethanol) and observed using a microscope.

Colony-forming assay

For the colony-forming assay, 5.0×10^3 cells per well were plated onto 6-well plates. After 7 days, colonies were stained with crystal violet staining solution (0.5% crystal violet, 3.7% formaldehyde, and 30% ethanol). The number of colonies was counted using the ImageJ program.

Immunoprecipitation assay

Immunoprecipitation (IP) was performed using Dynabeads Protein A and G (Thermo). Cells were washed with ice-cold PBS twice and lysed with ice-cold Pierce IP Lysis Buffer (Thermo) with protease inhibitor cocktail (Roche). After 5 min of incubation and 10 min of centrifugation at ~13,000*g*, the supernatants were transferred to another tube. The supernatants were precleared with 50 μl of Dynabeads Protein A and G for 1 h at 4°C. Primary antibodies were added to precleared supernatants, and the mixtures were incubated overnight at 4°C. The antibodies used for IP are listed in Supplementary Table S3. Then, 50 μl of Dynabeads Protein A and G were added to the samples, and the mixtures were incubated for 2 h at 4°C. The beads were subsequently washed twice. The immunoprecipitated proteins were eluted from the beads using 2× SDS sample buffer with or without glycerol and bromophenol blue (120 mM Tris-HCl [pH 6.8], 20% glycerol, 4% SDS, 28.8 mM β-mercaptoethanol, and 0.01% bromophenol blue).

Phosphatase activity assay

Phosphatase activity assays were performed using the Serine/Threonine Phosphatase Assay System (Promega, USA) according to the manufacturer's instructions.

Silver staining

Silver staining was performed using the PowerStain Silver Stain Kit (Elpisbiotech, Korea) according to the manufacturer's instructions.

High-throughput ELISA-based antibody array analysis

High-throughput enzyme-linked immunosorbent assay (ELISA)-based antibody array analysis was performed using a Phospho Explorer Antibody Array (Full Moon BioSystems) according to the manufacturer's instructions.

In vivo study

For the subcutaneous mouse model, cells were injected into the hip area on both sides of each mouse. Tumor growth was measured two times a week using an electronic caliper to measure two diameters using the following formula: length × width^2 × 0.5. The mean tumor volume at the start of the experiment was approximately 100 mm^3. Mice were sacrificed 7.5 weeks after the cell injections. The tumors were extracted, pooled for each experimental group, and mechanically disaggregated using steel operating scissors. Prism 7 (GraphPad Software, USA) was used for analysis.

All animal experiments were conducted in accordance with protocols approved by the Institutional Animal Care and Use Committee of the National Cancer Center, Republic of Korea (NCC-15-268).

In-solution protease digestion and peptide separation

The IP samples were precipitated using cold acetone, reduced with 10 mM DTT and alkylated by iodoacetamide (IAA). The alkylated samples were digested with mass spectrometry (MS)-grade Trypsin/Lys-C mix (Promega) in 50 mM Tris-HCl (pH 8) for 12 h at 37°C. Digested peptides were evaporated using a vacuum concentrator, separated using a high pH reversed-phase peptide fractionation kit (Thermo) and cleaned using C18 spin columns (Thermo) for MS analysis.

LC-MS/MS analysis

The peptides were analyzed on a Q Exactive HF-X Hybrid Quadrupole-Orbitrap mass spectrometer (Thermo) coupled with an Ultimate 3000 RSLCnano system (Thermo). The peptides were loaded onto a trap column (100 μm × 2 cm) packed with Acclaim PepMap100 C18 resin on which loaded peptides were eluted with a linear gradient from 5% to 28% solvent B (0.1% formic acid in ACN) for 110 min at a flow rate of 300 nl/min. The eluted peptides, separated by the analytical column (EASY-Spray column, 75 μm × 50 cm; Thermo), were sprayed into the nano-ESI source with an electrospray voltage of 2.1 kV. The Q Exactive HF-X Orbitrap mass analyzer was operated in top 20 data-dependent method. Full MS scans were acquired over the range m/z 350 to 1,800 with a mass resolution of 60,000 (at m/z 200). The AGC target value was 3.00E+06. The twenty most intense peaks with a charge state ≥ 2 were fragmented in the higher energy collisional dissociation (HCD) collision cell with a normalized collision energy of 28, and tandem mass spectra were acquired in the Orbitrap mass analyzer with a mass resolution of 15,000 at m/z 200.

Database searching of all raw data files was performed in Proteome Discoverer 2.2 software (Thermo). SEQUEST-HT was used for database searching against the SwissProt human database. Database searching against the corresponding reverse database was also performed to evaluate the false discovery rate (FDR) of peptide identification. The database searching parameters included a precursor ion mass tolerance of 10 ppm, a fragment ion mass tolerance of 0.08 Da, a fixed modification for carbamidomethyl cysteine (+57.021

Da/C) and variable modifications for methionine oxidation (+15.995 Da/M). We obtained an FDR of less than 1% on the peptide level and filtered with high peptide confidence.

Availability of data and material

The datasets used and/or analyzed during the current study are available within the manuscript and its supplementary information files.

RESULTS

High expression of PSPH is associated with the poor survival of lung cancer patients

To examine the association between PSPH expression and lung cancer progression, we collected and analyzed two public lung cancer gene expression datasets (GSE30219 and GSE37745) from the NCBI GEO database containing clinical information, including survival data (Botling et al., 2013; Rousseaux et al., 2013). Using the survival data, we examined the association between the survival of lung cancer patients and PSPH gene expression (Fig. 1A). The survival rate was significantly lower in the group with higher PSPH expression than the group with lower PSPH expression in both datasets (GSE30219: n = 293, $P = 0.0134$ for overall survival, $P = 0.00131$ for disease-free survival; GSE37745: n = 196, $P = 0.00822$ for overall survival, $P = 0.0252$ for recurrence-free survival, log-rank test) (Fig. 1A). Additionally, we examined the association between the survival of lung cancer patients and PSPH gene expression in other datasets, including The Cancer Genome Atlas (TCGA) lung cancer datasets (Supplementary Fig. S1). In the other datasets, the expression level of PSPH was also significantly associated with the survival of lung cancer patients. Then, we examined how frequently the PSPH gene was altered among lung cancer patients. We queried PSPH gene alterations in lung cancer from the TCGA database using the cBioPortal program (Figs. 1B and 1C). Approximately 3% to 7% of lung cancer patients had a copy number alteration (CNA) at the PSPH locus with gene amplification (Fig. 1B), and the CNA correlated with the PSPH expression level (Fig. 1C), with approximately 15% to 22% of lung cancer patients showing increased PSPH expression (Fig. 1B). Thus, we suggest that PSPH is frequently amplified in lung cancer and that the expression level is associated with cancer progression.

PSPH promotes *in vitro* lung cancer cell invasion and colony formation

Based on the association between PSPH expression and the prognosis of lung cancer patients, we examined lung cancer cell invasion and colony formation *in vitro* by modulating PSPH expression. The expression of PSPH was knocked down using siRNAs in two lung cancer cell lines, A549 and NCI-H1299, and the knockdown efficiency of PSPH was measured using the RT-qPCR assay (Fig. 2A). PSPH was successfully knocked down in A549 and NCI-H1299 cells (A549: $P = 4.8 \times 10^{-4}$ for siPSPH #1, $P = 4.8 \times 10^{-4}$ for siPSPH #2; NCI-H1299: $P = 1.4 \times 10^{-4}$ for siPSPH #1, $P = 3.1 \times 10^{-6}$ for siPSPH #2; *t*-test). Then, we performed invasion assays with lung cancer cells after treatment with two siRNAs for PSPH and a control siRNA. We found that PSPH knockdown significantly decreased the invasion ability in A549 and NCI-H1299 cells (Fig. 2B) (A549: $P = 2.7 \times 10^{-7}$ for siPSPH #1, $P = 3.7 \times 10^{-7}$ for siPSPH #2; NCI-H1299: $P = 5.8 \times 10^{-5}$ for siPSPH #1, $P = 2.3 \times 10^{-5}$ decrease for siPSPH #2; *t*-test). We performed colony-forming assays with lung cancer cells after treatment with two siRNAs for PSPH and a control siRNA. PSPH knockdown also significantly decreased the colony formation of A549 and NCI-H1299 cells (Fig. 2C) (A549: $P = 1.2 \times 10^{-3}$ for siPSPH #1, $P = 2.7 \times 10^{-4}$ for siPSPH #2; NCI-H1299: $P = 1.6 \times 10^{-4}$ for siPSPH #1, $P = 1.7 \times 10^{-4}$ for siPSPH #2; *t*-test). For reciprocal validation, we ectopically overexpressed His-tagged PSPH in the lung cancer cells, and the expression was validated using an immunoblot assay (Fig. 2D). His-tagged PSPH was successfully overexpressed in A549 and NCI-H1299 cells. Then, we performed invasion assays with the His-tagged PSPH-overexpressing lung cancer cells and the control cells. We found that ectopic PSPH overexpression significantly increased the invasion ability in A549 and NCI-H1299 cells (Fig. 2E) (A549: $P = 2.1 \times 10^{-8}$; NCI-H1299: $P = 5.4 \times 10^{-5}$; *t*-test). We performed colony-forming assays with the His-tagged PSPH-overexpressing lung cancer cells and the control cells. Ectopic PSPH overexpression also significantly increased the colony formation of A549 and NCI-H1299 cells (Fig. 2F) (A549: $P = 7.4 \times 10^{-3}$; NCI-H1299: $P = 4.1 \times 10^{-3}$; *t*-test). Thus, we suggest that PSPH promotes lung cancer invasion and colony formation, which are important processes for lung cancer progression.

Previous reports have shown that PSPH promotes cancer progression independently of the L-serine synthesis pathway (Bachelor et al., 2011). To examine whether the functions of PSPH in lung cancer are also independent of the L-serine synthesis pathway, we compared the effects of PSPH knockdown on invasion and colony formation with or without L-serine treatment (Figs. 2B and 2C). L-serine treatment had little effects effect on invasion and colony formation. Thus, we suggest that PSPH promotes lung cancer invasion and colony formation not through the L-serine synthesis pathway but through other noncanonical pathways.

IRS-1 is a putative target of dephosphorylation by PSPH

We hypothesized that PSPH could dephosphorylate phospho-serines in peptide sequences and tried to validate the phosphatase activity of PSPH on phospho-serines in peptide sequences (Fig. 3A). We precipitated PSPH and its interacting proteins from PSPH-overexpressing and control cells using either a His-tag antibody or a PSPH antibody, and then we measured the peptide-dephosphorylating activity of these immunoprecipitated samples (Fig. 3A). Immunoprecipitated samples from PSPH-overexpressing cells had higher phosphatase activity on phospho-peptide. Thus, we suggest that PSPH can dephosphorylate not only phospho-L-serine but also other phospho-peptides.

To identify the phospho-proteins regulated by PSPH, we performed high-throughput ELISA-based antibody array analysis following PSPH knockdown and treatment with control siRNAs in lung cancer cells (Fig. 3B and Supplementary Table S4). The phosphorylation of 42 proteins was decreased by PSPH knockdown. Under the hypothesis that PSPH would

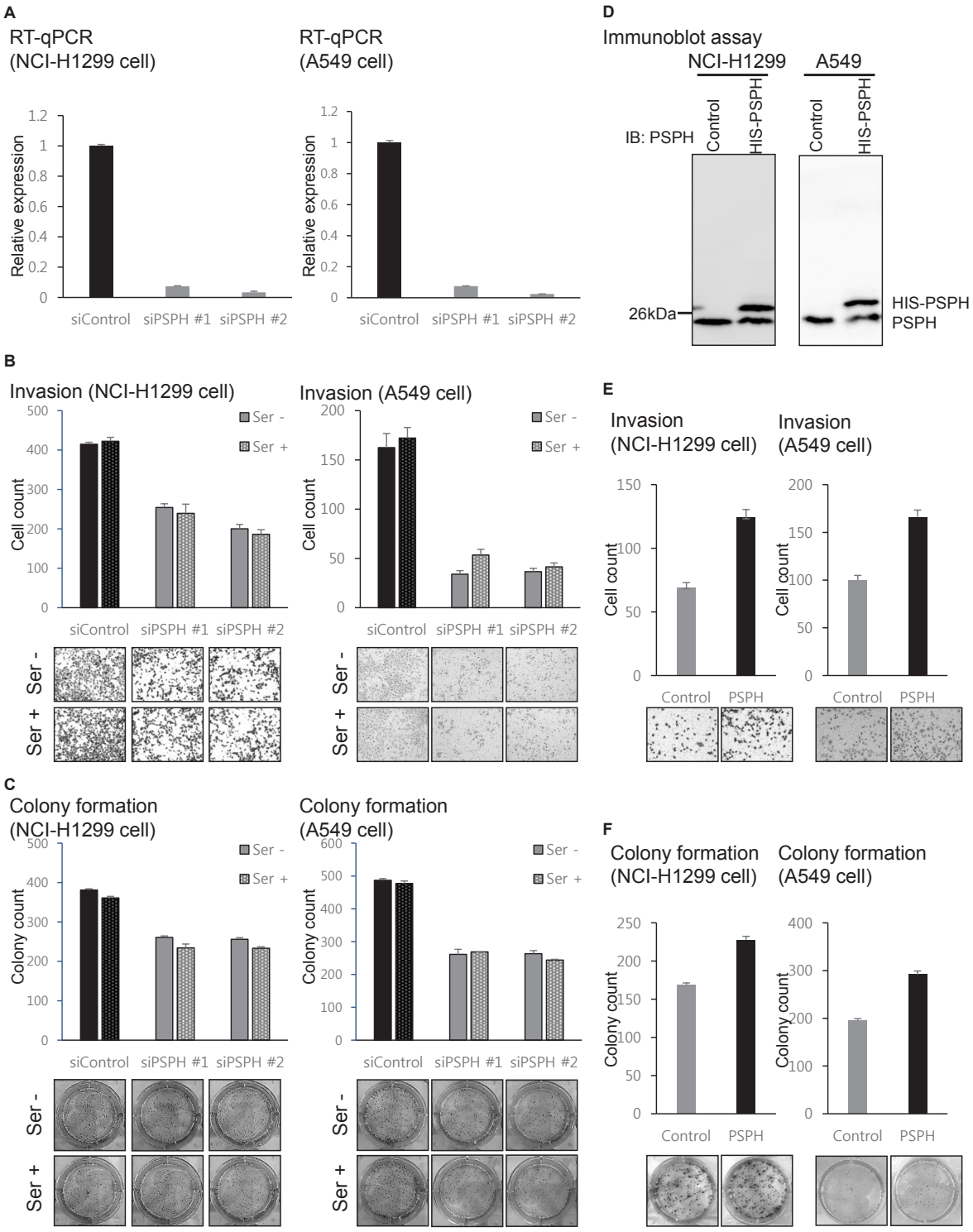

Fig. 2. Promotion of lung cancer cell invasion and colony formation by PSPH *in vitro*. After PSPH knockdown: RT-qPCR (A), invasion assay (B), and colony-forming assay (C). After ectopic PSPH overexpression: immunoblot assay (D), invasion assay (E), and colony-forming assay (F). Data are representative of three independent experiments. The error bars represent the standard error of the mean.

dephosphorylate phospho-serines in peptide sequences, we focused on serine phosphorylation; then, 22 phospho-proteins were selected as putative PSPH targets (Fig. 3B). From the protein phosphorylation profile, we found that phospho-serines in several proteins associated with well-known signaling pathways (insulin, nuclear factor-kappa B, mTOR, MAP

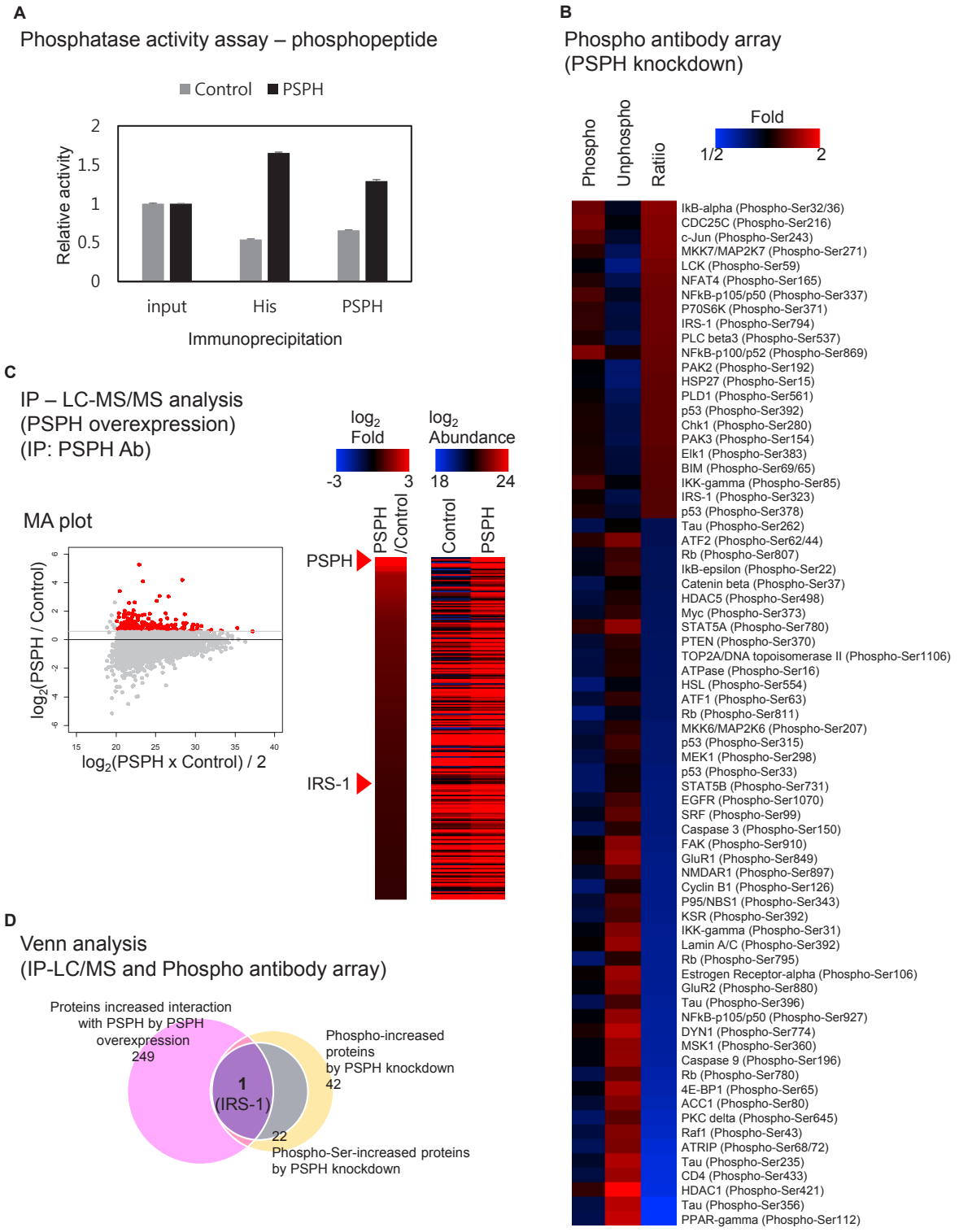

Fig. 3. Regulation of protein phosphorylation by PSPH. (A) Phosphatase activity assay on phosphopeptides using PSPH IP samples. Data are representative of three independent experiments. The error bars represent the standard error of the mean. (B) Differentially (serine-) phosphorylated proteins by PSPH knockdown (high-throughput ELISA-based phosphoantibody array). (C) LC-MS/MS analysis with PSPH IP samples. (D) Venn analysis with the LC-MS/MS and phosphoantibody array data.

kinase pathways, etc.) were regulated by PSPH (Fig. 3B).

To identify the proteins that physically interact with PSPH, we performed IP with PSPH- or His-tag-specific antibodies, SDS-PAGE and silver staining in the His-tagged PSPH-overexpressing lung cancer cells and the control cells (Supplementary Fig. S2). We detected a specific interaction between PSPH and an ~180 kDa-sized protein in ectopic His-tagged PSPH-overexpressing A549 and NCI-H1299 cells (Supplementary Fig. S2). Based on the protein size (~180 kDa) and the serine-phosphorylated candidate proteins from the antibody array data (Fig. 3B and Supplementary Fig. S2), we found that only one protein, insulin receptor substrate 1 (IRS-1), could be a candidate for a direct target protein of PSPH.

We also tried to identify proteins that physically interact with PSPH in lung cancer cells. We performed liquid chromatography-mass spectrometry (LC-MS/MS) analysis after immunoprecipitating PSPH and its interacting proteins from PSPH-overexpressing and control cells using the PSPH antibody (Fig. 3C). We detected 252 proteins with an increased interaction with PSPH after overexpressing PSPH in lung cancer cells (Supplementary Table S5). A Venn analysis of the antibody array data and LC-MS/MS analysis data (Figs. 3B and 3C) revealed a putative PSPH target protein, IRS-1, which is a well-known regulator of insulin signaling (Fig. 3D). Thus, we suggest that PSPH promotes lung cancer invasion and colony formation potentially through IRS-1 dephosphorylation.

PSPH activates IRS-1 and downstream signaling

To validate the physical interaction between PSPH and IRS-1, we performed immunoblot (IB) assays with PSPH-specific IP samples of the PSPH-overexpressing lung cancer cells and the control cells (Fig. 4A). The results showed the specific interaction between PSPH and IRS-1 in A549 and NCI-H1299 lung cancer cells. To determine whether PSPH regulates IRS-1 dephosphorylation, after normalizing the amount of IRS-1 with the PSPH-specific IP samples, we performed immunoblot assays using an anti-phospho-serine antibody (Fig. 4B). We found that ~25% of phospho-serine on an ~180 kDa-sized protein (the same size as IRS-1) was decreased by PSPH overexpression. Thus, we confirmed that PSPH physically interacts with IRS-1 and that PSPH regulates IRS-1 dephosphorylation.

Then, we further examined IRS-1 dephosphorylation by PSPH. To determine which phospho-serine sites of IRS-1 could be dephosphorylated by PSPH, we performed immunostaining with phospho-IRS-1-specific antibodies after PSPH overexpression or knockdown (Fig. 4C and Supplementary Fig. S3). As a result, we found that the phosphorylation of serine 794 (Ser794) of IRS-1 was dephosphorylated by PSPH overexpression (Fig. 4C) and phosphorylated by PSPH knockdown (Supplementary Fig. S3) in lung cancer cells. To examine whether a well-known active site, aspartic acid 20 (D20), of PSPH is essential for IRS-1 phosphorylation, we generated a PSPH mutant clone whose aspartic acid 20 was substituted to the alanine of PSPH (D20A). Consequently, we performed immunostaining with phospho-IRS-1(Ser794)-specific antibodies after D20A mutant overexpression in lung cancer cells and compared the results to those of the wild type (Fig. 4C). IRS-1 Ser794 was dephosphorylated by PSPH overexpression, but D20A PSPH overexpression did not affect IRS-1 Ser794. These results imply that IRS-1 Ser794 is a direct substrate of PSPH and that the D20 of PSPH is the active site not only for the phospho-amino acid serine but also for the phospho-serine in the IRS-1 protein sequence.

IRS-1 Ser794 is reported as an inhibitory phosphorylation site that inhibits IRS-1 activity and downstream signaling pathways, including Akt phosphorylation and activity (Tzatsos and Tsichlis, 2007). Therefore, we examined whether the downstream signaling pathway of IRS-1 was influenced by PSPH (Fig. 4D). Downstream signaling-specific antibodies were used to perform immunoblot assays with the wild type and D20A mutant PSPH-overexpressing lung cancer cells and the control cells (Fig. 4D). We found that wild type PSPH increased the phosphorylation of Akt serine 473 (pAkt S473) and p70 S6 kinase serine 371 (pS6K S371), but D20A mutant PSPH did not. These phosphorylation sites are known as active phosphorylation sites that activate Akt and p70 S6 kinase, which are regulators of phosphoinositide 3-kinase (PI3K) and mammalian target of rapamycin (mTOR) signaling (Magnuson et al., 2012; Risso et al., 2015). Then, we examined the downstream target genes of the Akt signaling pathway. We performed RT-qPCR assays using specific primers for the known downstream target genes of the Akt signaling pathway in PSPH over-expressed and control lung cancer cells (Fig. 4E). The expressions of the known target genes were significantly increased by ectopic PSPH overexpression (CDK2: $P = 4.0 \times 10^{-5}$, HRAS: $P = 7.0 \times 10^{-5}$, MAPKAP1: $P = 8.0 \times 10^{-4}$, SLC2A1: $P = 1.4 \times 10^{-6}$; *t*-test). To verify the target gene regulation by PSPH in clinical samples, we also examined the correlations between PSPH and the downstream target genes using the public datasets which were used for previous analysis, GSE30219 and GSE37745 (Fig. 4F and Supplementary Fig. S4). As we expected, the expressions of the known Akt target genes were positively and significantly correlated with PSPH expression in clinical samples. To examine whether the downstream change of phospho-Akt by PSPH induced significant functional changes in lung cancer or not, we performed invasion assays with rapamycin treatment, which was well-known mTOR inhibitor, after ectopic PSPH overexpression (Fig. 4G). The result showed that the mTOR inhibition by rapamycin decreased the invasion abilities of lung cancer cells which were increased by PSPH (NCI-H1299: $P = 5.8 \times 10^{-5}$, A549: $P = 7.4 \times 10^{-5}$; *t*-test). These results all imply that PSPH regulates lung cancer progression through the insulin-PI3K-Akt-mTOR signaling axis.

PSPH promotes lung cancer progression *in vivo* and in clinical samples

To examine PSPH functions *in vivo*, we used a mouse xenograft model. We performed subcutaneous injection with PSPH-knockdown cells and control cells and observed the tumor size and weight (Figs. 5A-5C). PSPH knockdown caused a decrease in both tumor size and weight. An IRS-1 Ser794-specific antibody was used to perform IHC staining with the tumor tissues from mouse xenografts (Fig. 5D). We found that PSPH knockdown caused an increase in IRS-1 Ser794 in the tumor tissues. Then, we examined the expressions of PSPH and phospho-IRS-1 in clinical samples (Fig. 5E). We performed IHC assays with the tissue microarrays of lung

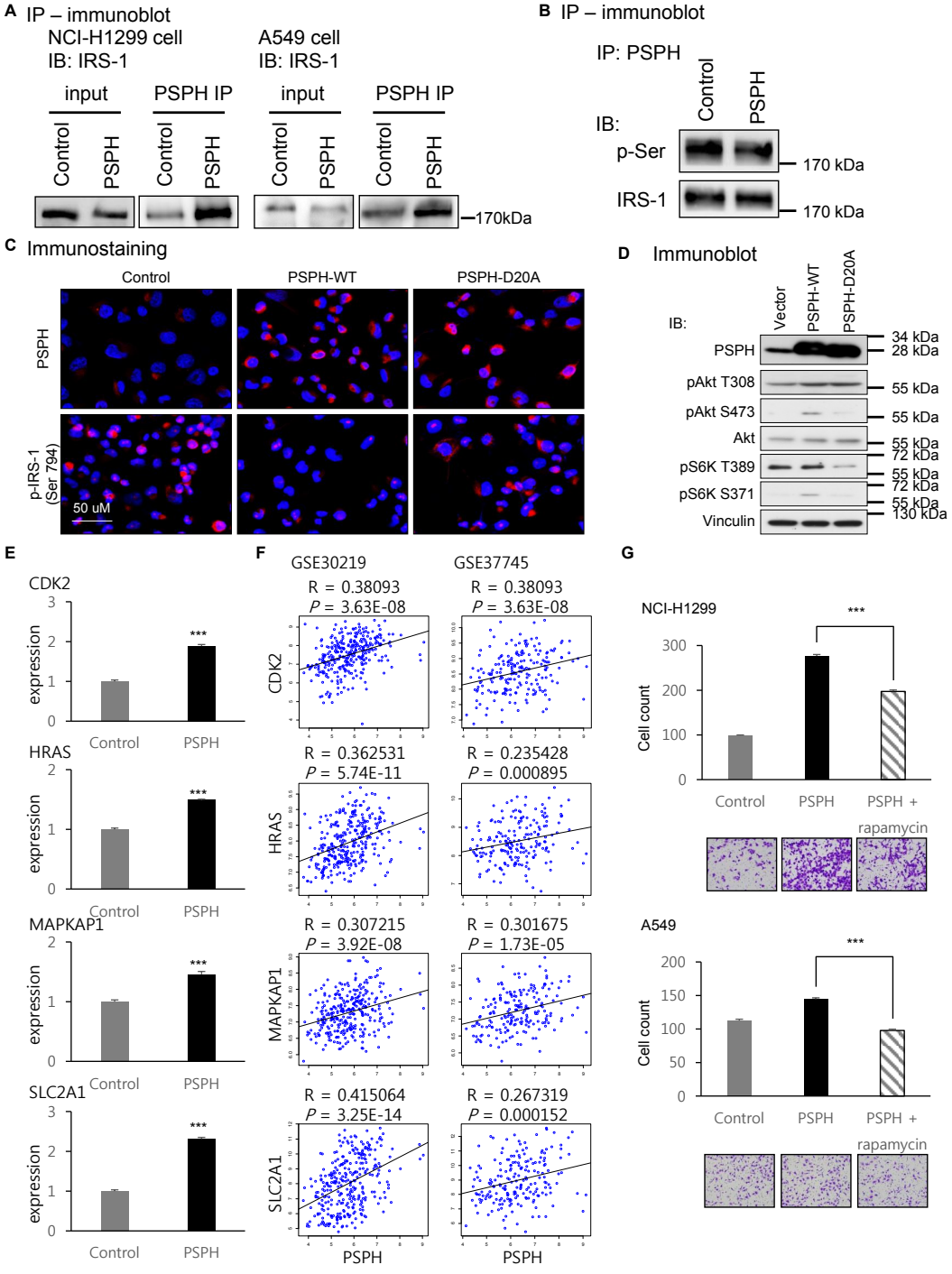

Fig. 4. Regulation of IRS-1 phosphorylation and downstream signals by PSPH. (A) Validation of the specific interaction between PSPH and IRS-1 proteins. (B) Validation of IRS-1 dephosphorylation by PSPH overexpression (immunoblot assay). (C) Validation of IRS-1 dephosphorylation by wild type (WT) and mutant (D20A) PSPH (immunostaining). Red, phospho-IRS-1 (Ser794); Blue, DAPI. (D) Regulation of downstream signals by WT and mutant (D20A) PSPH. (E) Results of the RT-qPCR assay for the known downstream target genes of the Akt signaling pathway (CDK2: $P = 4.0 \times 10^{-5}$, HRAS: $P = 7.0 \times 10^{-5}$, MAPKAP1: $P = 8.0 \times 10^{-4}$, SLC2A1: $P = 1.4 \times 10^{-6}$; *t*-test). (F) The correlation between PSPH and Akt target genes. (G) The results of invasion assays with rapamycin treatment after ectopic PSPH overexpression (NCI-H1299: $P = 5.8 \times 10^{-5}$, A549: $P = 7.4 \times 10^{-5}$; *t*-test). Data are representative of three independent experiments. The error bars represent the standard error of the mean. $***P < 0.001$.

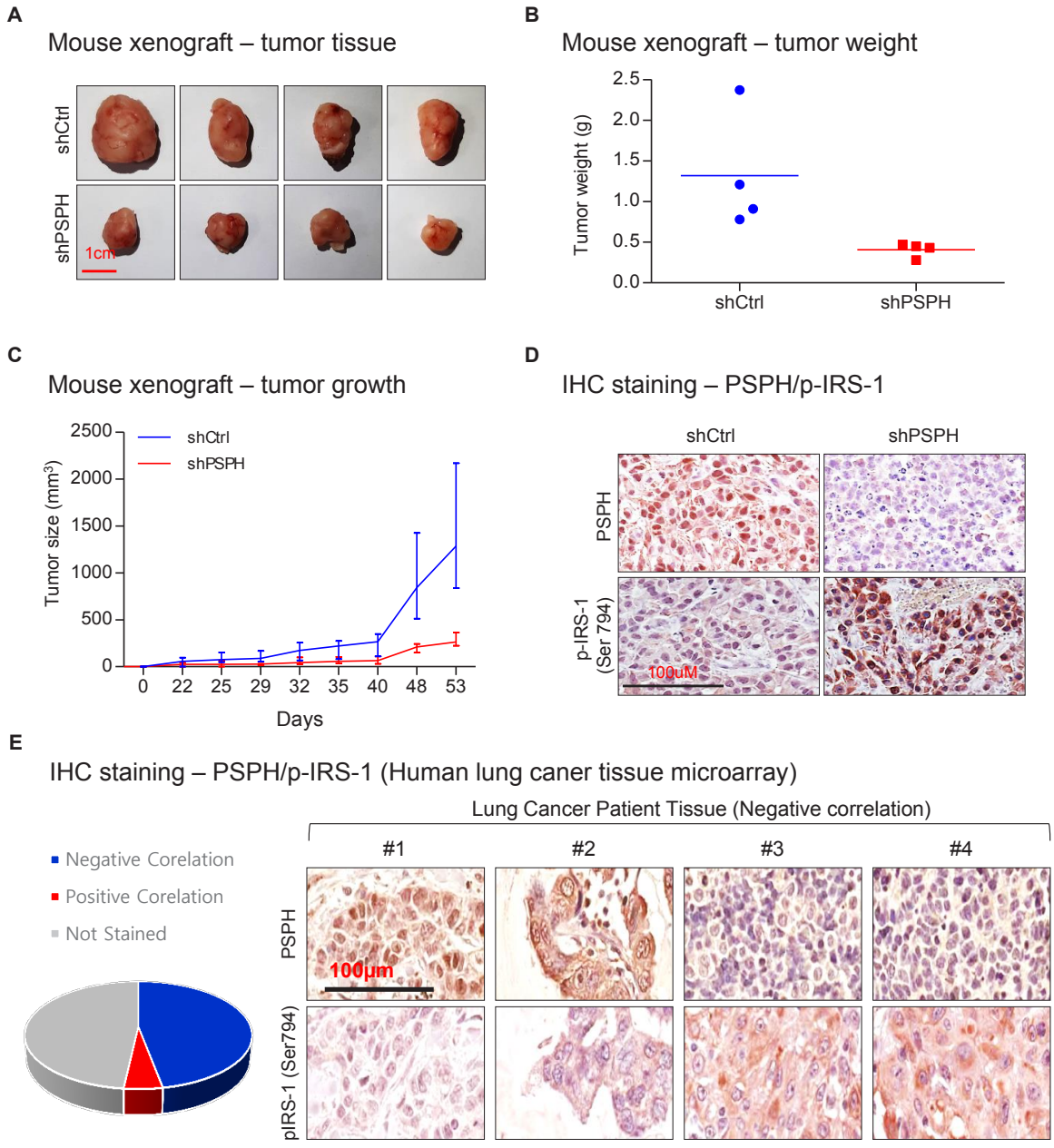

Fig. 5. Regulation of lung cancer by PSPH *in vivo*. Mouse xenograft after PSPH knockdown: tumor volume (A), tumor weight (B), and tumor size (the error bars represent the standard deviation of the mean) (C). (D) Result of the IHC staining with tumor tissues of mouse xenograft model. (E) Result of the IHC staining with lung cancer tissue microarray.

cancer patients as below. The results showed that the most of stained tissues with PSPH- or phospho-IRS-1 Ser794-specific antibodies showed negative correlation (negative: 40 cancer tissues, positive: 4 cancer tissues) between PSPH expression and IRS-1 phosphorylation. These results all imply that the regulation of lung cancer through IRS-1 dephosphorylation by PSPH also occurs *in vivo* and in clinical sample.

DISCUSSION

Our study showed that PSPH was significantly associated with the prognosis of lung cancer patients and promoted the invasion and colony formation of lung cancer cells independent of L-serine synthesis. PSPH bound to the IRS-1 protein to dephosphorylate phospho-serine in the protein sequences and regulates the insulin-PI3K-mTOR signaling axis.

Metabolism in cancer is closely related with other cancer-related functions (Jeong and Haigis, 2015; Kim, 2018). Amino acid starvation, especially essential amino acid starvation, sensitizes drug sensitivity in various cancers (Maddocks et al., 2017; Saito et al., 2018). The limitation of L-serine, a nonessential amino acid, also sensitizes drug sensitivity in

several cancers, such as lymphoma, leukemia and liver and intestinal cancers, but it is not effective on lung cancer (https://www.biorxiv.org/content/10.1101/281253v1) (Maddocks et al., 2017). Lung cancer appears to be insensitive to L-serine concentration considering results from previous studies and ours. Nevertheless, PSPH, an enzyme involved in L-serine metabolism, shows a serious association with lung cancer phenotype. Our study began with the curiosity of these phenomena.

The expression of PSPH is regulated by various factors, such as c-Myc activation (Sun et al., 2015), estrogen regulation (Lee et al., 2015) and testosterone regulation (Sanborn et al., 1975). In lung cancer, CNA appears to be one of the major factors of PSPH overexpression, because the copy number of the PSPH gene is frequently amplified and correlates with the expression level in lung cancer according to the TCGA lung cancer data. Considering that PSPH overexpression repeatedly presents a significant association with a poor prognosis of lung cancer patients in various datasets, we believe that CNA and PSPH expression have potential as robust markers for lung cancer prognosis.

Similar to PSPH functions in SCC (Bachelor et al., 2011), the knockdown of PSPH decreased the invasion and colony formation of lung cancer cells, but adding an excess of serine did not rescue the invasion and colony formation phenotypes according to our study, suggesting that at least two cancer types are regulated by PSPH expression through noncanonical L-serine-independent pathways. Because previous studies reported an association between PSPH and various cancer types, such as SCC, lung, gastric, breast, brain, and colon cancers (Bachelor et al., 2011; Hemmati et al., 2003; Herzfeld et al., 1978; Maddocks et al., 2013; Pollari et al., 2011; Shimomura et al., 2004; Tan et al., 2010), we believe that finding other PSPH functions in the noncanonical L-serine-independent pathways would be of interest for functional and therapeutic studies in various cancers.

In this study, we focused on one putative target of PSPH dephosphorylation, IRS-1. However, we showed that PSPH could dephosphorylate phospho-serine/threonine in the peptide sequence and provided a list of putative targets from LC-MS/MS analysis and the high-throughput ELISA-based antibody array experiment. These data show other PSPH targets of noncanonical L-serine-independent pathways. Our LC-MS/MS analysis data represent the whole proteome of PSPH-interacting proteins. Our antibody array data refine the proteome data, with ~1,300 probes from hundreds of proteins. Therefore, the Venn analysis (Fig. 3D) represents a restricted set of all putative PSPH target proteins. Additional phosphoproteome analysis data could provide other putative PSPH target proteins.

IRS-1 contains ~70 potential serine/threonine sites, and various serine/threonine kinases are known to phosphorylate these residues (Morino et al., 2006). However, the mechanism of IRS-1 dephosphorylation and the related phosphatases are not well known. Our study revealed a novel upstream phosphatase of IRS-1, PSPH, which dephosphorylates Ser794. Most phosphatases have a passive mode of action (unlike kinases), indicating that phosphatases attenuate protein functions by reversing the activation functions of kinases. Interestingly, PSPH has an active mode of action to activate IRS-1 through inhibitory Ser794 dephosphorylation and influences the insulin-PI3K-mTOR signaling axis. Therefore, we found a novel mode of action of a phosphatase.

Although metabolic enzymes are not good targets for cancer treatment in general, a few specific metabolic pathways, such as glycolysis and glutamine metabolism, are aberrantly dysregulated in cancer and are good targets for cancer treatment (DeBerardinis and Cheng, 2010; Metallo et al., 2011; Moreno-Sanchez et al., 2007; Shanware et al., 2011; Warburg, 1956). The glycolytic metabolic enzyme pyruvate kinase M2 (PKM2) is famous for directly regulating tyrosine-phosphorylated peptides in cancer instead of glycolysis (Christofk et al., 2008a; 2008b). Similar to PKM2, PSPH regulates a representative metabolic pathway of glycolytic intermediates: the serine metabolic pathway (Possemato et al., 2011). According to our results PSPH also regulates serine-phosphorylated peptides. While targeting metabolic PSPH has limitations for therapeutics, targeting the specific interaction between PSPH and serine-phosphorylated proteins can be a potential therapeutic approach of metabolic inhibitory therapy. Therefore, we suggest that our results offer a potentially novel therapeutic option for lung cancer patients by blocking the interplay between PSPH and IRS-1.

Note: Supplementary information is available on the Molecules and Cells website (www.molcells.org).

Disclosure

The authors have no potential conflicts of interest to disclose.

ACKNOWLEDGMENTS

This work was supported by grants from the Basic Science Research Program through the National Research Foundation of Korea (NRF) funded by the Ministry of Science and ICT (NRF-2015R1C1A1A02037583 to S.-M.P., NRF-2018R1C1B6004768 to J.Y., and NRF-2017MBA9B5060884 to S.-Y.K) and KRIBB research initiative grant.

We thank the Proteomics Core Facility at the National Cancer Center in Korea, which provided mass spectrometry services.

ORCID

Seong-Min Park https://orcid.org/0000-0002-5064-0503
Eun-Hye Seo https://orcid.org/0000-0003-3265-794X
Dong-Hyuck Bae https://orcid.org/0000-0002-1511-0558
Sung Soo Kim https://orcid.org/0000-0001-9214-9379
Jina Kim https://orcid.org/0000-0002-1532-1320
Weiwei Lin https://orcid.org/0000-0001-7894-5408
Kyung-Hee Kim https://orcid.org/0000-0002-7623-3949
Jong Bae Park https://orcid.org/0000-0003-0207-0697
Yong Sung Kim https://orcid.org/0000-0001-7113-272X
Jinlong Yin https://orcid.org/0000-0003-3143-7240
Seon-Young Kim https://orcid.org/0000-0002-1030-7730

REFERENCES

Amelio, I., Cutruzzola, F., Antonov, A., Agostini, M., and Melino, G. (2014). Serine and glycine metabolism in cancer. Trends Biochem. Sci. *39*, 191-

198.

Anderson, D.D., Woeller, C.F., Chiang, E.P., Shane, B., and Stover, P.J. (2012). Serine hydroxymethyltransferase anchors de novo thymidylate synthesis pathway to nuclear lamina for DNA synthesis. J. Biol. Chem. *287*, 7051-7062.

Bachelor, M.A., Lu, Y., and Owens, D.M. (2011). L-3-Phosphoserine phosphatase (PSPH) regulates cutaneous squamous cell carcinoma proliferation independent of L-serine biosynthesis. J. Dermatol. Sci. *63*, 164-172.

Borkenhagen, L.F. and Kennedy, E.P. (1958). The enzymic equilibration of L-serine with O-phospho-L-serine. Biochim. Biophys. Acta *28*, 222-223.

Botling, J., Edlund, K., Lohr, M., Hellwig, B., Holmberg, L., Lambe, M., Berglund, A., Ekman, S., Bergqvist, M., Ponten, F., et al. (2013). Biomarker discovery in non-small cell lung cancer: integrating gene expression profiling, meta-analysis, and tissue microarray validation. Clin. Cancer Res. *19*, 194-204.

Christofk, H.R., Vander Heiden, M.G., Harris, M.H., Ramanathan, A., Gerszten, R.E., Wei, R., Fleming, M.D., Schreiber, S.L., and Cantley, L.C. (2008a). The M2 splice isoform of pyruvate kinase is important for cancer metabolism and tumour growth. Nature *452*, 230-233.

Christofk, H.R., Vander Heiden, M.G., Wu, N., Asara, J.M., and Cantley, L.C. (2008b). Pyruvate kinase M2 is a phosphotyrosine-binding protein. Nature *452*, 181-186.

Collet, J.F., Gerin, I., Rider, M.H., Veiga-da-Cunha, M., and Van Schaftingen, E. (1997). Human L-3-phosphoserine phosphatase: sequence, expression and evidence for a phosphoenzyme intermediate. FEBS Lett. *408*, 281-284.

Collet, J.F., Stroobant, V., Pirard, M., Delpierre, G., and Van Schaftingen, E. (1998). A new class of phosphotransferases phosphorylated on an aspartate residue in an amino-terminal DXDX(T/V) motif. J. Biol. Chem. *273*, 14107-14112.

Collet, J.F., Stroobant, V. and Van Schaftingen, E. (1999). Mechanistic studies of phosphoserine phosphatase, an enzyme related to P-type ATPases. J. Biol. Chem. *274*, 33985-33990.

DeBerardinis, R.J. and Cheng, T. (2010). Q's next: the diverse functions of glutamine in metabolism, cell biology and cancer. Oncogene *29*, 313-324.

de Koning, T.J., Snell, K., Duran, M., Berger, R., Poll-The B.T., and Surtees, R. (2003). L-serine in disease and development. Biochem. J. *371*, 653-661.

Douillard, J.Y., Rosell, R., De Lena, M., Carpagnano, F., Ramlau, R., Gonzales-Larriba, J.L., Grodzki, T., Pereira, J.R., Le Groumellec, A., Lorusso, V., et al. (2006). Adjuvant vinorelbine plus cisplatin versus observation in patients with completely resected stage IB-IIIA non-small-cell lung cancer (Adjuvant Navelbine International Trialist Association [ANITA]): a randomised controlled trial. Lancet Oncol. *7*, 719-727.

Hemmati, H.D., Nakano, I., Lazareff, J.A., Masterman-Smith, M., Geschwind, D.H., Bronner-Fraser, M., and Kornblum, H.I. (2003). Cancerous stem cells can arise from pediatric brain tumors. Proc. Natl. Acad. Sci. U. S. A. *100*, 15178-15183.

Herzfeld, A., Legg, M.A., and Greengard, O. (1978). Human colon tumors: enzymic and histological characteristics. Cancer *42*, 1280-1283.

Hoffman, P.C., Mauer, A.M., and Vokes, E.E. (2000). Lung cancer. Lancet *355*, 479-485.

Jeong, S.M. and Haigis, M.C. (2015). Sirtuins in cancer: a balancing act between genome stability and metabolism. Mol. Cells *38*, 750-758.

Kalhan, S.C. and Hanson, R.W. (2012). Resurgence of serine: an often neglected but indispensable amino acid. J. Biol. Chem. *287*, 19786-19791.

Kim, J.A. (2018). Cooperative instruction of signaling and metabolic pathways on the epigenetic landscape. Mol. Cells *41*, 264-270.

Lee, J.Y., Lim, W., Jo, G., Bazer, F.W., and Song, G. (2015). Estrogen regulation of phosphoserine phosphatase during regression and recrudescence of female reproductive organs. Gen. Comp. Endocrinol. *214*, 40-46.

Locasale, J.W. (2013). Serine, glycine and one-carbon units: cancer metabolism in full circle. Nat. Rev. Cancer *13*, 572-583.

Lund, K., Merrill, D.K., and Guynn, R.W. (1985). The reactions of the phosphorylated pathway of L-serine biosynthesis: thermodynamic relationships in rabbit liver in vivo. Arch. Biochem. Biophys. *237*, 186-196.

Maddocks, O.D., Berkers, C.R., Mason, S.M., Zheng, L., Blyth, K., Gottlieb, E., and Vousden, K.H. (2013). Serine starvation induces stress and p53-dependent metabolic remodelling in cancer cells. Nature *493*, 542-546.

Maddocks, O.D.K., Athineos, D., Cheung, E.C., Lee, P., Zhang, T., van den Broek, N.J.F., Mackay, G.M., Labuschagne, C.F., Gay, D., Kruiswijk, F., et al. (2017). Modulating the therapeutic response of tumours to dietary serine and glycine starvation. Nature *544*, 372-376.

Magnuson, B., Ekim, B., and Fingar, D.C. (2012). Regulation and function of ribosomal protein S6 kinase (S6K) within mTOR signalling networks. Biochem. J. *441*, 1-21.

Metallo, C.M., Gameiro, P.A., Bell, E.L., Mattaini, K.R., Yang, J., Hiller, K., Jewell, C.M., Johnson, Z.R., Irvine, D.J., Guarente, L., et al. (2011). Reductive glutamine metabolism by IDH1 mediates lipogenesis under hypoxia. Nature *481*, 380-384.

Moreno-Sanchez, R., Rodriguez-Enriquez, S., Marin-Hernandez, A., and Saavedra, E. (2007). Energy metabolism in tumor cells. FEBS J. *274*, 1393-1418.

Morino, K., Petersen, K.F., and Shulman, G.I. (2006). Molecular mechanisms of insulin resistance in humans and their potential links with mitochondrial dysfunction. Diabetes *55* Suppl 2, S9-S15.

Nesbitt, J.C., Putnam, J.B., Jr., Walsh, G.L., Roth, J.A., and Mountain, C.F. (1995). Survival in early-stage non-small cell lung cancer. Ann. Thorac. Surg. *60*, 466-472.

Neuhaus, F.C. and Byrne, W.L. (1958). O-Phosphoserine phosphatase. Biochim. Biophys. Acta *28*, 223-224.

Pignon, J.P., Tribodet, H., Scagliotti, G.V., Douillard, J.Y., Shepherd, F.A., Stephens, R.J., Dunant, A., Torri, V., Rosell, R., Seymour, L., et al. (2008). Lung adjuvant cisplatin evaluation: a pooled analysis by the LACE Collaborative Group. J. Clin. Oncol. *26*, 3552-3559.

Pollari, S., Kakonen, S.M., Edgren, H., Wolf, M., Kohonen, P., Sara, H., Guise, T., Nees M., and Kallioniemi, O. (2011). Enhanced serine production by bone metastatic breast cancer cells stimulates osteoclastogenesis. Breast Cancer Res. Treat. *125*, 421-430.

Possemato, R., Marks, K.M., Shaul, Y.D., Pacold, M.E., Kim, D., Birsoy, K., Sethumadhavan, S., Woo, H.K., Jang, H.G., Jha, A.K., et al. (2011). Functional genomics reveal that the serine synthesis pathway is essential in breast cancer. Nature *476*, 346-350.

Risso, G., Blaustein, M., Pozzi, B., Mammi, P., and Srebrow, A. (2015). Akt/PKB: one kinase, many modifications. Biochem. J. *468*, 203-214.

Roselli, M., Mariotti, S., Ferroni, P., Laudisi, A., Mineo, D., Pompeo, E., Ambrogi, V., and Mineo, T.C. (2006). Postsurgical chemotherapy in stage IB nonsmall cell lung cancer: long-term survival in a randomized study. Int. J. Cancer *119*, 955-960.

Ross, K.C., Andrews, A.J., Marion, C.D., Yen, T.J., and Bhattacharjee, V. (2017). Identification of the serine biosynthesis pathway as a critical component of BRAF inhibitor resistance of melanoma, pancreatic, and non-small cell lung cancer cells. Mol. Cancer Ther. *16*, 1596-1609.

Rousseaux, S., Debernardi, A., Jacquiau, B., Vitte, A.L., Vesin, A., Nagy-Mignotte, H., Moro-Sibilot, D., Brichon, P.Y., Lantuejoul, S., Hainaut, P., et al. (2013). Ectopic activation of germline and placental genes identifies aggressive metastasis-prone lung cancers. Sci. Transl. Med. *5*, 186ra166.

Saito, Y., Moriya, S., Kazama, H., Hirasawa, K., Miyahara, K., Kokuba, H., Hino, H., Kikuchi, H., Takano, N., Hiramoto, M., et al. (2018). Amino acid starvation culture condition sensitizes EGFR-expressing cancer cell lines to gefitinib-mediated cytotoxicity by inducing atypical necroptosis. Int. J. Oncol. *52*, 1165-1177.

Sanborn, T.A., Kowle, R.L., and Sallach, H.J. (1975). Regulation of enzymes of serine and one-carbon metabolism by testosterone in rat prostate, liver, and kidney. Endocrinology *97*, 1000-1007.

Shanware, N.P., Mullen, A.R., DeBerardinis, R.J., and Abraham, R.T. (2011). Glutamine: pleiotropic roles in tumor growth and stress resistance. J. Mol. Med. *89*, 229-236.

Shimomura, K., Sakakura, C., Takemura, M., Takagi, T., Fukuda, K., Kin, S., Nakase, Y., Miyagawa, K., Ohgaki, M., Fujiyama, J., et al. (2004). Combination of L-3-phosphoserine phosphatase and CEA using real-time RT-PCR improves accuracy in detection of peritoneal micrometastasis of gastric cancer. Anticancer Res. *24*, 1113-1120.

Siegel, R., Naishadham, D., and Jemal, A. (2013). Cancer statistics, 2013. CA Cancer J. Clin. *63*, 11-30.

Strunck, E., Frank, K., Tan, M.I., and Vollmer, G. (2001). Expression of l-3-phosphoserine phosphatase is regulated by reconstituted basement membrane. Biochem. Biophys. Res. Commun. *281*, 747-753.

Sun, L., Song, L., Wan, Q., Wu, G., Li, X., Wang, Y., Wang, J., Liu, Z., Zhong, X., He, X., et al. (2015). cMyc-mediated activation of serine biosynthesis pathway is critical for cancer progression under nutrient deprivation conditions. Cell Res. *25*, 429-444.

Tabatabaie, L., Klomp, L.W., Berger, R., and de Koning, T.J. (2010). L-serine synthesis in the central nervous system: a review on serine deficiency disorders. Mol. Genet. Metab. *99*, 256-262.

Tan, E.H., Ramlau, R., Pluzanska, A., Kuo, H.P., Reck, M., Milanowski, J., Au, J.S., Felip, E., Yang, P.C., Damyanov, D., et al. (2010). A multicentre phase II gene expression profiling study of putative relationships between tumour biomarkers and clinical response with erlotinib in non-small-cell lung cancer. Ann. Oncol. *21*, 217-222.

Tedeschi, P.M., Markert, E.K., Gounder, M., Lin, H., Dvorzhinski, D.S., Dolfi, C., Chan, L.L., Qiu, J., DiPaola, R.S., Hirshfield, K.M., et al. (2013). Contribution of serine, folate and glycine metabolism to the ATP, NADPH and purine requirements of cancer cells. Cell Death Dis. *4*, e877.

Tzatsos, A. and Tsichlis, P.N. (2007). Energy depletion inhibits phosphatidylinositol 3-kinase/Akt signaling and induces apoptosis via AMP-activated protein kinase-dependent phosphorylation of IRS-1 at Ser-794. J. Biol. Chem. *282*, 18069-18082.

van der Linden, I.J., Heil, S.G., van Egmont Petersen, M., van Straaten, H.W., den Heijer, M., and Blom, H.J. (2008). Inhibition of methylation and changes in gene expression in relation to neural tube defects. Birth Defects Res. A Clin. Mol. Teratol. *82*, 676-683.

Vazquez, A., Tedeschi, P.M., and Bertino, J.R. (2013). Overexpression of the mitochondrial folate and glycine-serine pathway: a new determinant of methotrexate selectivity in tumors. Cancer Res. *73*, 478-482.

Warburg, O. (1956). On the origin of cancer cells. Science *123*, 309-314.

Winton, T., Livingston, R., Johnson, D., Rigas, J., Johnston, M., Butts, C., Cormier, Y., Goss, G., Inculet, R., Vallieres, E., et al. (2005). Vinorelbine plus cisplatin vs. observation in resected non-small-cell lung cancer. N. Engl. J. Med. *352*, 2589-2597.

Wood, P.L., Hawkinson, J.E., and Goodnough, D.B. (1996). Formation of D-serine from L-phosphoserine in brain synaptosomes. J. Neurochem. *67*, 1485-1490.